

Pseudo Exclusive-OR for LDPC Coded Two-Way Relay Block Fading Channels

Jianquan Liu[†], Meixia Tao[†], Youyun Xu^{†*}

[†]Dept. of Electronic Engineering, Shanghai Jiao Tong University, Shanghai, 200240, China

*PLA University of Science and Technology, Nanjing 210007, China

Emails: {jianquanliu, mxtao, xuyouyun}@sjtu.edu.cn

Abstract—We present a new adaptive physical layer network coding (PLNC) method, called *pseudo exclusive-or* (PXOR), for LDPC coded two-way relay (TWR) block fading channels. Based on the pairwise check decoding (PCD) we proposed earlier, the check relationship table generated by the PXOR mapping obtains the same Hamming distances of the PLNC mapped codewords as that of conventional XOR mapping. In the meantime, the PXOR mapping optimizes the Euclidean distances by adjusting the symbol distances dynamically in order to compensate the amplitude fading and phase deviation due to channel fading. Simulation results on system end-to-end error probability show that the proposed PXOR considerably outperforms the conventional XOR while achieving the same performance as the closest-neighbor cluster with much lower complexity.

I. INTRODUCTION

With the advent of physical layer network coding (PLNC), two-way relaying increases the spectral efficiency of wireless cooperative networks efficiently [1]–[6]. In terms of capacity deduction of two-way relay (TWR) channels, the achievable rate regions based on full decoding [7], [8] and partial decoding [9], [10] have been reported recently. It is known that partial decoding is capable of achieving a larger rate region as opposed to full decoding. Particularly, compared with traditional amplify-and-forward (AF) and decode-and-forward (D-F) protocols, the denoise-and-forward (DNF) protocol, a type of partial decoding, has demonstrated significant performance gain [11]. Consequently, the realization of partial decoding by practical coding and modulation techniques remains to be a fundamental and challenging task.

Recently, two kinds of partial decoding realizations, conventional XOR [12]–[14] and arithmetic-sum [15], have been reported for TWR Gaussian channels based on certain linear codes. Note that both methods are designed specifically for symmetric and Gaussian channels. For TWR channel with fading, the conventional XOR does not always work well due to the undesired phase and amplitude offset between the two channels in multiple-access (MA) phase. Authors in [16] therefore proposed an adaptive PLNC mapping with respect to the instantaneous channel fading, named as closest-neighbor cluster (CNC) mapping. To further ensure reliable communication, the authors extended this method for convolutional-coded

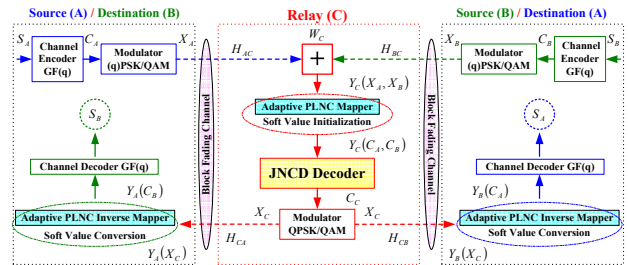


Fig. 1: Channel coding model for TWR block fading channels.

system in [17] and discussed the code design based on trellis-coded modulation (TCM). However, it requires to change the coding structure at the two source nodes and adapt between two transmission protocols.

In our earlier work [18], we extended the adaptive PLNC mapping CNC to LDPC (low density parity check) coded TWR block fading channels, and proposed the pairwise check decoding (PCD) based on the symbol distance priority maximization (SDPM). The generated check relationship table (check-relation-tab) (denoted as PCD(I)) is, however, enormous usually and not easy to optimize due to the shattered pairwise check constraints.

In this paper, we introduce an alternative partial decoding, using the Hamming distance priority maximization (HDPM) based on PCD, for LDPC coded TWR block fading channels. In this regard, we propose a new adaptive PLNC mapping, called *pseudo exclusive-or* (PXOR). It preserves the same Hamming distance of the generated check-relation-tab (named as PCD(II)) as that of the conventional XOR mapping and obtains approximately the same symbol distance as the CNC mapping. For the system end-to-end (ETE) error probability, simulation results show that the proposed coded PXOR mapping with PCD(II) considerably outperforms the coded conventional XOR mapping with belief propagation (BP) and achieves the same performance as the complicated coded CNC mapping with PCD(I) for two TWR block fading channels.

II. CHANNEL CODING MODEL FOR TWR CHANNELS

We consider a TWR fading channel where two source nodes, denoted as A and B , exchange information with the help of a relay node, denoted as C . We assume that all the nodes operate in the half-duplex mode. The channel on each communication link is assumed to be corrupted with block fading and additive white Gaussian noise (AWGN). For

This work is supported by the NSF of China under grant 60902019, the Joint Research Fund for Overseas Chinese, Hong Kong and Macao Young Scholars under grant 61028001, and the Innovation Program of Shanghai Municipal Education Commission under grant 11ZZ19.

simplicity, we also assume the channel gains are reciprocal and unchanged during a whole packet transmission.

The proposed channel coding is illustrated in Fig. 1, where the communication takes place in two phases. First, the information packet from each source, denoted as \mathbf{S}_i , for $i \in \{A, B\}$, is encoded individually by a traditional LDPC code with parity check matrix \mathbf{H}_i . Unlike the existing work, we do not impose the constraint that \mathbf{H}_A and \mathbf{H}_B must be identical. Instead, we only require that they have the same size and the same location of non-zero elements. We further assume that the encoder is operated in $\mathbf{GF}(q)$, where $q \in \{2^1, 2^2, 2^3, \dots\}$. Note that q -ary ($q > 2$) coding could improve the performance compared with binary coding. The encoded packet, \mathbf{C}_i , is modulated by using q -ary modulation, such as q -PSK or q -QAM, generating \mathbf{X}_i , and then transmitted simultaneously to the relay node. The n -th symbol of each packet is denoted as $\mathbf{C}_i(n) \in \mathcal{Z}_q$, $\mathcal{Z}_q = \{0, 1, \dots, q-1\}$, and $\mathbf{X}_i(n) \in \mathcal{Q}_q$, respectively. The superimposed packet received by the relay, denoted as \mathbf{Y}_C is given by

$$\mathbf{Y}_C = H_{AC}\mathbf{X}_A + H_{BC}\mathbf{X}_B + \mathbf{W}_C, \quad (1)$$

where $H_{i'j}$ denotes the complex-valued channel coefficient of link from node i to node i' , and $\mathbf{W}_{i'}$ denotes complex AWGN with variance $\sigma_{i'}^2$ of node i' . Therein, $\{i, i'\} \in \{A, B, C\}$.

We assume perfect symbol synchronization at the two sources and perfect channel estimation at the relay. After receiving the superimposed packet, the relay first computes the probability of the adaptive PLNC mapped coded symbol pair, denoted as $\mathbf{C}_C = \mathcal{M}(\mathbf{C}_A, \mathbf{C}_B)$, based on the instantaneous channel states during the MA phase, then obtains their hard-decision using the JNCD decoder, the details of which have been presented in [18]. Here, \mathcal{M} denotes a certain adaptive PLNC mapping, see for example the CNC mapping in [16]. Note that no full decoding of \mathbf{C}_A and \mathbf{C}_B as an intermediate step is needed. No extra channel encoding at the relay is needed either. Then, the relay broadcasts the modulated coded symbols of \mathbf{C}_C , denoted as \mathbf{X}_C , and mapping rule $\mathcal{M}()$ to two source nodes. The received signals at the nodes A and B are respectively written as

$$\mathbf{Y}_A = H_{CA}\mathbf{X}_C + \mathbf{W}_A; \mathbf{Y}_B = H_{CB}\mathbf{X}_C + \mathbf{W}_B. \quad (2)$$

Each source node computes the probability of the desired information $\mathbf{C}_A(\mathbf{C}_B)$ from the received symbols $\mathbf{Y}_B(\mathbf{Y}_A)$ by using the adaptive PLNC mapping rule with the help of its self-information $\mathbf{C}_B(\mathbf{C}_A)$. Lastly, the traditional LDPC decoding algorithm, e.g. BP, is applied, the output of which is the desired information packet $\mathbf{S}_A(\mathbf{S}_B)$. Note that each source node should know the check matrix of the other source.

III. ANALYSIS OF OUTAGE PROBABILITY

In this section, we derive the system outage probability of TWR fading channel, which serves as a good approximation of the achievable frame error rate (FER) in the limit of infinite block length [19]. Here, the system is said to be in outage if the achievable sum-rate falls below a target. Since the capacity region of two-way relaying with partial decoding is

still unknown [9], [10], we resort to the capacity outer bound as follows [8, Theorem 2], based on which a lower bound of the outage probability can be obtained.

$$(R_{AB}, R_{BA}) : \begin{cases} R_{AB} \leq \min(\beta C_{AC}, (1-\beta)C_{CB}), \\ R_{BA} \leq \min(\beta C_{BC}, (1-\beta)C_{CA}) \end{cases} \quad (3)$$

where β is the time sharing parameter, R_{ij} and C_{ij} are denoted as the instantaneous data rate and channel capacity of the link from node i to node j , for $i, j \in \{A, B, C\}$, respectively.

Let us further assume that the TWR channels considered here are reciprocal, i.e. $C_{ij} = C_{ji}$ for $i, j \in \{A, B, C\}$. From (3), we can easily obtain the upper bound of the maximum sum-rate for the considered TWR channels

$$S_u = \max_{(R_{AB}, R_{BA}) \in (3)} R_{AB} + R_{BA} = \min(C_{AC}, C_{BC}), \quad (4)$$

which is also given in [11]. Therein, each of the terms C_{ij} , $i, j \in \{A, B, C\}$, is the channel capacity of a traditional point-to-point channel with input alphabet $x_{ij} \in \mathcal{Q}_q$ and received signal $y_{ij} = \alpha_{ij}x_{ij} + w_{ij}$, where $w_{ij} \sim \mathcal{N}(0, \sigma^2)$ and α_{ij} denotes a real- or complex-valued channel coefficient of the link from node i to j with $\mathbb{E}\{|\alpha_{ij}^2|\} = 1$.

With the further assumption of equiprobable channel inputs, extending the well-known formula for the capacity of continuous-valued Gaussian channels [20, Eqs. 3-5] to the case of block fading channels yields

$$C_{ij}(\alpha_{ij}) = \log_2(q) - \frac{1}{q} \sum_{m=0}^{q-1} \mathbb{E} \left\{ \log_2 \sum_{n=0}^{q-1} \exp \left[-\frac{|y_{ij} - \alpha_{ij}x_{ij}^n|^2 - |y_{ij} - \alpha_{ij}x_{ij}^m|^2}{2\sigma^2} \right] \right\} \quad (5)$$

in bit/channel use. Here, \mathbb{E} represents expectation over y_{ij} given $x_{ij} = x_{ij}^m$ and α_{ij} , where x_{ij}^m or x_{ij}^n is an element of the modulated signal sets $\{\mathcal{Q}_q : x_{ij}^0, x_{ij}^1, \dots, x_{ij}^{q-1}\}$.

In addition, we denote the data rate r_{ij} as the average spectral efficiency of the link from node i to node j , $\{i, j\} \in \{A, B\}$, and the target rate of overall system as $S_r = r_{AB} + r_{BA}$. Then, we have

$$\begin{aligned} S_r &= \beta \left(R_{AB} \log_2^{qAB} + R_{BA} \log_2^{qBA} \right) \\ &= \frac{1}{2} \left(R \log_2^q + R \log_2^q \right) = R \log_2^q, \end{aligned} \quad (6)$$

where R is denoted as the channel code rate. Then the outage probability can be lower bounded as

$$\begin{aligned} P_{out} &\geq P(S_u < S_r) \\ &= P\left(\min \left\{ C_{AC}(\alpha_{AC}), C_{BC}(\alpha_{BC}) \right\} < S_r \right), \end{aligned} \quad (7)$$

which can be easily evaluated by Monte Carlo averaging over the block fading coefficients and the AWGN.

IV. PROPOSED PSEUDO EXCLUSIVE-OR MAPPING (PXOR)

Since the CNC mapping tries to maximize the symbol distance, it is unavoidable that the dimension of CNC mapped symbols may violate traditional channel coding theory (Galois field) by using the SDPM. Although we have proposed an

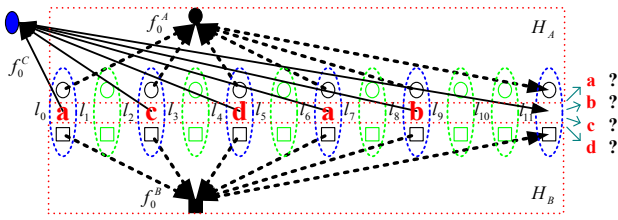


Fig. 2: Tanner graph of check function versus symbol pairs at relay.

exhaustive search optimization in [18], the size of the desired check-relation-tab for PCD decoder (named as PCD(I)) usually grows exponentially with the row weight and is not easy to be optimized due to the irregular dimension of the CNC mapped symbols. In this work we introduce an alternative partial decoding by using the HDPM based on the PCD. In this regard, the check-relation-tab (named as PCD(II)) generated by the one-to-one correlation optimization (OCO) is proposed and a new PXOR mapping is presented.

A. One-to-one correlation optimization (OCO)

Similar to [18], the PCD algorithm will be suitable for use if we know the check functions of symbol pairs at the relay. As an example, we derive the check function of f_0^C for a virtual LDPC code at the relay from f_0^A and f_0^B ($f_0^A \in \mathbf{H}_A$, $f_0^B \in \mathbf{H}_B$) using the segmental Tanner graph in Fig. 2, where the code length is 12 and the row weight and column weight are 6 and 3 respectively. The solid circles and squares denote the check functions, while non-solid ones denote the transmitted symbols at each source node. Likewise, the solid and non-solid ellipses denote the check functions and the corresponding received symbol pairs. f_r^s denote the r -th check function of the LDPC code at node s , where $r \in [0, 5]$, $s \in \{A, B, C\}$. l_n denotes the symbol pair $(\mathbf{C}_A(n), \mathbf{C}_B(n))$, for $n \in [0, 11]$.

We can see that the table size of Tab.II in [18] is far away from the minimum value $q^{l(r_k-1)}$ and the weighted factors F_W are always not equal to 1, where r_k and q^l denote the k -th row weight of the applied check matrixes and the range of PLNC mapped symbols, $q \leq q^l \leq q^2$, respectively. These phenomena decrease the Hamming distance of the desired codewords, which is undesired. Then, we introduce an OCO method to generate check-relation tabs, as shown in Tabs. I and II. Here, one-to-one correlation between any two elements of the four possible values $\{a, b, c, d\}$ is realized, which is same to the check-relation tabs generated by the conventional XOR. Note that we may not achieve the one-to-one relationship even through the exhausting search optimization if five possible values $\{a, b, c, d, e\}$ are mapped, as described in [18]. Obviously, Tab.II here has a very small size $4^{(r_k-1)}$ compared to that of [18] (approaching 5^{r_k}) if $\mathbf{GF}(4)$ LDPC codes are applied at two source nodes.

B. Theoretical principles for PXOR mapping

Since the conventional XOR mapping preserves the codeword space for linear codes but is restricted to static mapping, we shall propose the PXOR mapping, which obtains the same Hamming distance as the conventional XOR mapping

TABLE I: Check-relation-tab of f_0^C for virtual encoder if $q = 2^2$

	(0, 0)	(2, 2)	(4, 4)	(6, 6)	(8, 8)	(11, 11)
\mathcal{M}_1	a	a	a	a	a	a
\mathcal{M}_2	a	a	a	a	b	b
\mathcal{M}_3	a	a	a	a	c	c
\mathcal{M}_4	a	a	a	a	d	d
\mathcal{M}_5	:	:	:	:	:	:
\mathcal{M}_6	d	d	d	d	c	c
1024×6	d	d	d	d	d	d

TABLE II: Check-relation-tab of f_0^C for PCD decoder if $q = 2^2$

	(11, 11)	F_W	(0, 0)	(2, 2)	(4, 4)	(6, 6)	(8, 8)
\mathcal{M}_1	a	1	a	a	a	a	a
\mathcal{M}_2	a	1	a	a	a	b	b
\mathcal{M}_3	a	1	a	a	a	c	c
\mathcal{M}_4	a	1	a	a	a	d	d
\mathcal{M}_5	:	:	:	:	:	:	:
\mathcal{M}_6	d	1	d	d	d	c	c
1024×7	d	1	d	d	d	d	d

and maps dynamically according to the block fading channel coefficient, in order to maximize the MED. For linear block codes \mathbf{H}_A and \mathbf{H}_B , if all row weights are even and all non-zero elements in identical rows are the same, then we have the following theorems.

Theorem 1: Any one of the q clusters, composed by the random symbol pairs based on the exclusive law [16], can be mapped to any one of the q distinct symbols.

Theorem 2: All possible q clusters, composed by randomly exchanging any q distinct symbols of one node $A(B)$, generate the identical codeword space.

Corollary 2.1: There are $\frac{1}{q} \mathcal{P}_q^q$ kinds of possible q clusters satisfying the Theorem 2, where \mathcal{P} denotes permutation.

The proofs of these theorems and corollary are straightforward and here omitted.

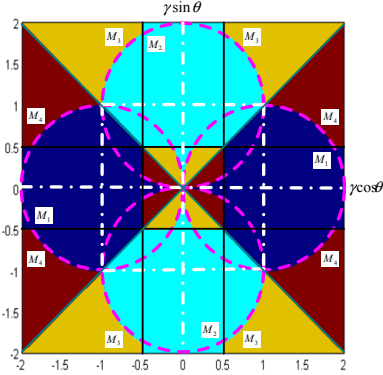
For example, 4 clusters $\{(0, 0), (1, 1), (2, 2), (3, 3)\}$, $\{(0, 1), (1, 0), (2, 3), (3, 2)\}$, $\{(0, 2), (1, 3), (2, 0), (3, 1)\}$ and $\{(0, 3), (1, 2), (2, 1), (3, 0)\}$ can be mapped to any one of 24 order permutations from the conventional XOR mapped symbols $\{0, 1, 2, 3\}$ according to the Theorem 1 when $q = 2^2$. Namely, 4 clusters can be randomly mapped to $\{0, 1, 2, 3\}$, $\{0, 1, 3, 2\}$, $\{0, 2, 1, 3\}$ and relatives. Accordingly, we pick up 4 columns $[0, 1, 2, 3]'$, $[1, 0, 3, 2]'$, $[2, 3, 0, 1]'$, $[3, 2, 1, 0]'$, which are q distinct symbols of one node $A(B)$, from the former 4 clusters. Arbitrarily exchanging two columns among the aforementioned 4 columns, we obtain 5 additional kinds of PXOR mapping excluding the base clusters following the Theorem 2. Lastly, 6 clusters can be generated by the PXOR mapping, as shown in Tab. III. To avoid confusion, we let $\{a, b, c, d\}$ indicate the broadcasted symbols $\{1, 2, 3, 4\}$.

C. Network coding design based on PXOR mapping

This subsection focuses on maximizing the symbol distance to optimize the MED under the constraint of no any loss in Hamming distance. By assuming that all symbols in $\mathbf{GF}(q)$ have same probability of occurrence, each symbol pair is

TABLE III: Adaptive PXOR mapping for 4-ary LDPC codes

	(0, 0)(0, 1)(0, 2)(0, 3)	(1, 0)(1, 1)(1, 2)(1, 3)	(2, 0)(2, 1)(2, 2)(2, 3)	(3, 0)(3, 1)(3, 2)(3, 3)
\mathcal{M}_1	a b c d	b a d c	c d a b	d c b a
\mathcal{M}_2	a b c d	c d a b	b a d c	d c b a
\mathcal{M}_3	a b c d	d c b a	b a d c	c d a b
\mathcal{M}_4	a b c d	d c b a	c d a b	b a d c
\mathcal{M}_5	a b c d	c d a b	d c b a	b a d c
\mathcal{M}_6	a b c d	b a d c	d c b a	c d a b


 Fig. 3: Adaptive PXOR mapping according to the channel ratio $H_{BC}/H_{AC} = \gamma(\cos\theta + j\sin\theta)$ when $q = 2^2$.

also generated with the same probability when the length of codeword tend to infinite. Then, optimizing the MED between q modulated PXOR mapped symbols is equivalent to optimize the MED between any two modulated PXOR mapped codewords approximatively.

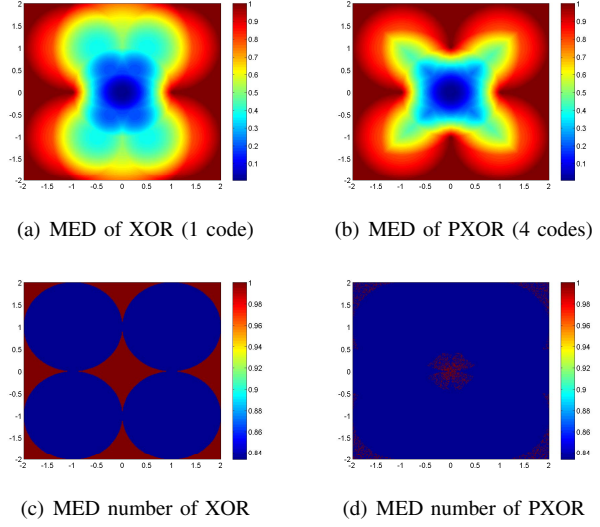
Data: given $\gamma, \theta, q, \mathcal{M}_i, i \in [1, \frac{1}{q}\mathcal{P}_q]$

Result: Network coding rule based on PXOR mapping

- 1 Compute MED d_{min}^i and number $N_{d_{min}^i}$ of symbol pairs with MED among all \mathcal{M}_i mapped symbols;
- 2 Select maximum value $V_{d_{min}}$ from $\{d_{min}^i, i \in [1, \frac{1}{q}\mathcal{P}_q]\}$;
- 3 **if** $d_{min}^i = d_{min}^j = V_{d_{min}}, i \neq j$ **then**
- 4 Select minimum value $V_{N_{d_{min}}}$ from $\{N_{d_{min}^i}, N_{d_{min}^j}\}$;
- 5 **if** $N_{d_{min}^i} = V_{N_{d_{min}}}$ **then**
- 6 Select \mathcal{M}_i
- 7 **else**
- 8 Select \mathcal{M}_j
- 9 **end**
- 10 **else**
- 11 **if** $d_{min}^i = V_{d_{min}}$ **then**
- 12 Select \mathcal{M}_i
- 13 **end**
- 14 **end**

Algorithm 1: Network coding design for PXOR mapping

According to Algorithm 1, network coding rule based on the PXOR mapping (listed in Tab. III) is depicted in Fig. 3. Note that \mathcal{M}_5 and \mathcal{M}_6 are omitted, it is because that they could not increase the MED or decrease the number of symbol pairs with the MED (also named as MED number) although they maybe increase sub MED compared to \mathcal{M}_3 and \mathcal{M}_4 respectively. Moreover, optimized MED by the PXOR mapping and the conventional XOR mapping are presented, as depicted in Fig. 4(a,b). Therein, all MEDs are normalized by $1.6568 \times (4 + 4\sqrt{2})|\mathbf{H}_{AC}|^2$, where $(4 + 4\sqrt{2})$ is the


 Fig. 4: Normalized MED and number of symbol pairs with MED versus channel ratio $\mathbf{H}_{BC}/\mathbf{H}_{AC}$ when $q = 2^2$ (x-axis: $\gamma \cos\theta$, y-axis: $\gamma \sin\theta$, z-axis: $d_{min}(a,b), N_{d_{min}}(c,d)$).

MED when $\mathbf{H}_{AC} = \mathbf{H}_{BC} = 1$. Fig. 4(a, b) shows that the MEDs are increased generally except for the areas around the center when the PXOR mapping is applied. In addition, the MED numbers for two considered mapping are also produced, as depicted in Fig. 4(c,d). The MED number is normalized by $(1/3.6122) \log_2^{10}$. We can see that the MED number can decrease dramatically in the aforesaid areas around the center for the PXOR mapping from Fig. 4(c,d). Obviously, Fig. 4 confirms that the proposed PXOR mapping is an effective method for increasing the MED and decreasing the MED number. Note that the areas with the extremely small MED are shrunked quickly when the codeword length tends to infinite.

V. SIMULATION RESULTS

Suppose that the channel gains on all links follow Rayleigh or Rice distribution and are independent. We assume $E[|H_{AC}|^2] = E[|H_{BC}|^2] = 1$, where notation $E[\cdot]$ denotes expectation function. For simplicity, each node uses the same transmission power 1 and the same noise power σ^2 . Define an average SNR per information symbol as $\frac{1}{2R\sigma^2}$, where R is the code rate. The selection for the PXOR mapping is based on instantaneous realizations of the channel gain pairs $\{\mathbf{H}_{AC}, \mathbf{H}_{BC}\}$ using Fig. 3 while the CNC mapping using Fig.4 in [16]. In the simulation, the proposed PXOR with PCD(II) based on HDPM is employed. For comparison, three benchmark systems are considered. One is the uncoded case, where QPSK modulation is applied and the relay demodulates using different PLNC mappings. Another is the coded conventional XOR case, where the same codes are applied at two sources and relay performs traditional BP decoding based on conventional XOR. The other is CNC mapping with PCD(I) decoding at the relay based on SDPM [18]. The black solid lines, denoted as ‘‘Outage Probability’’, are actually the lower bound of the outage probability in (7). According to the theoretical principles for PXOR mapping, we generate a 4-ary

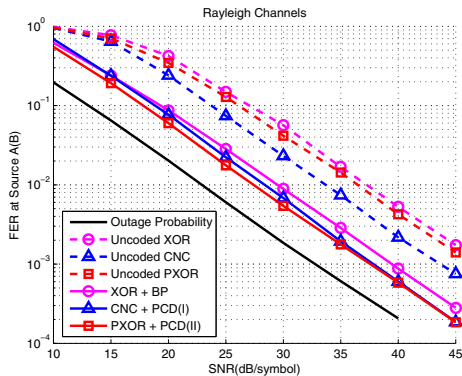


Fig. 5: Performance comparisons in Rayleigh channels.

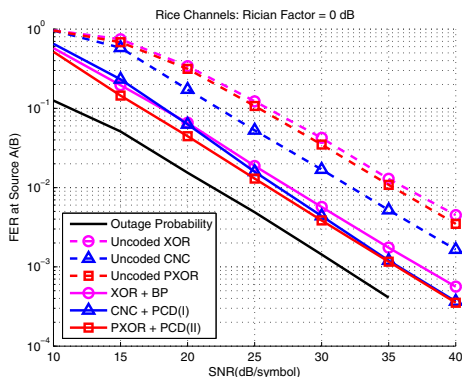


Fig. 6: Performance comparisons in Rice channels.

code from a binary LDPC codes "504.504.3.504", which is produced by MacKay [21], through replacing $\{1, \dots, 1\}$ by $\{\eta, \dots, \eta\}$, $\eta \in \mathcal{Z}_4$. Code length, code rate, row weight and column weight are 1008, 0.5, 6 and 3, respectively. Note that each simulated FER value is obtained after observing at least 100 error frames. The maximum iteration is 25.

Fig. 5 shows the ETE performance of the Rayleigh channels. For the three uncoded cases, the CNC outperforms the PXOR about 3 dB and the latter is better than the XOR about 1 dB at $\text{FER} = 1.8 \times 10^{-3}$. Moreover, the coding gains of the coded XOR and the coded PXOR are 8.5 dB and 9 dB, respectively. The coding gain of the coded CNC is 6 dB at $\text{FER} = 7.5 \times 10^{-4}$. We also see that both the coded PXOR and coded CNC outperform the coded XOR about 2 dB at $\text{FER} = 2.8 \times 10^{-4}$.

The similar observations can be made in Fig. 6 where the channel becomes Rice fading with the Rician factor 0 dB. For the three uncoded cases, the XOR is worse than the PXOR for about 1.2 dB while the latter is inferior to the CNC about 3.3 dB. At $\text{FER} = 4.8 \times 10^{-3}$, the coding gains of the coded XOR and the coded PXOR are 9.2 dB and 9.7 dB, respectively. We also observe that coded CNC has about 6.7 dB at $\text{FER} = 1.8 \times 10^{-3}$ in terms of coding gain. It is clear that both the coded CNC and the coded PXOR are better than the coded XOR about 1.7 dB at $\text{FER} = 5.8 \times 10^{-4}$.

VI. CONCLUSION

In this paper, we proposed a new PLNC at the relay, named as *pseudo exclusive-or*, or *PXOR*, for LDPC coded TWR

block fading channels. We randomly permute two columns from q clusters mapped by conventional XOR, $\frac{1}{q}P_q^q$ kinds of PXOR mapping are generated. By adaptively selecting these PXOR maps according to channel gains, the MED of received signals is optimized directly. Simulation results show that the proposed coded PXOR mapping significantly outperforms the coded conventional XOR and meanwhile achieves the same performance as the highly complex coded CNC mapping.

REFERENCES

- [1] Y. Wu, P. A. Chou, and S.-Y. Kung, "Information exchange in wireless networks with network coding and physical-layer broadcast," in *Proc. 39th Conf. Inform. Sciences Systems (CISS)*, Mar. 2005.
- [2] P. Popovski and H. Yomo, "Bi-directional amplification of throughput in a wireless multi-hop network," in *Proc. IEEE Veh. Tech. Conf. (VTC)*, May 2006, pp. 588–593.
- [3] C. Hausl and J. Hagenauer, "Iterative network and channel decoding for the two-way relay channel," in *Proc. IEEE Int. Conf. Comm. (ICC)*, Jun. 2006, pp. 1568–1573.
- [4] S. Zhang, S. C. Liew, and P. P. Lam, "Physical-layer network coding," in *Proc. ACM 15th Annual Int. Conf. Mobile Computing Networking (MobiCom)*, Sept. 2006, pp. 358–365.
- [5] S. Katti, H. Rahul, W. Hu, D. Katabi, M. M. edard, and J. Crowcroft, "XORs in the air: Practical wireless network coding," in *Proc. ACM SIGCOMM*, Sept. 2006, pp. 243–254.
- [6] B. Rankov and A. Wittneben, "Spectral efficient protocols for half-duplex fading relay channels," *IEEE Jour. Sel. Areas. Comm.*, vol. 25, no. 2, pp. 379–389, Feb. 2007.
- [7] T. J. Oechtering, C. Schnurr, I. Bjelakovic, and H. Boche, "Broadcast capacity region of two-phase bidirectional relaying," *IEEE Trans. Inform. Theory*, vol. 54, no. 1, pp. 454–458, Jan. 2008.
- [8] S. J. Kim, P. Mitran, and V. Tarokh, "Performance bounds for bi-directional coded cooperation protocols," *IEEE Trans. Inform. Theory*, vol. 54, no. 11, pp. 5235–5241, Nov. 2008.
- [9] C. Schnurr, S. Stanczak, and T. J. Oechtering, "Achievable rates for the restricted half-duplex two-way relay channel under a partial-decode-and-forward protocol," in *Proc. IEEE Inform. Theory Workshop (ITW)*, May 2008, pp. 134–138.
- [10] D. Gunduz, E. Tuncel, and J. Nayak, "Rate regions for the separated two-way relay channel," in *Proc. 46th Annual Allerton Conf. Comm. Control Computing*, Sept. 2008, pp. 1333–1340.
- [11] P. Popovski and H. Yomo, "Physical network coding in two-way wireless relay channels," in *Proc. IEEE Int. Conf. Comm. (ICC)*, June 2007, pp. 707–712.
- [12] W. Nam, S.-Y. Chung, and Y. H. Lee, "Capacity bounds for two-way relay channel," in *Proc. Int. Zurich Seminar Comm. (IZS)*, March 2008, pp. 144–147.
- [13] B. Nazer and M. Gastpar, "The case for structured random codes in network communication theorems," in *Proc. Inform. Theory Workshop (ITW)*, Sept. 2007.
- [14] K. Narayanan, M. P. Wilson, and A. Sprintson, "Joint physical layer coding and network coding for bi-directional relaying," in *Proc. Allerton Conf. Comm., Control and Computing*, 2007.
- [15] S. Zhang and S.-C. Liew, "Channel coding and decoding in a relay system operated with physical-layer network coding," *IEEE Jour. Sel. Areas. Comm.*, vol. 27, no. 5, pp. 788–796, June 2009.
- [16] T. Koike-Akino, P. Popovski, and V. Tarokh, "Optimized constellations for two-way wireless relaying with physical network coding," *IEEE Jour. Sel. Areas. Comm.*, vol. 27, no. 5, pp. 773–787, June 2009.
- [17] —, "Denosing strategy for convolutionally-coded bidirectional relaying," in *Proc. IEEE Int. Conf. Comm. (ICC)*, 2009.
- [18] J. Liu, M. Tao, Y. Xu, and X. Wang, "Pairwise check decoding for LDPC coded two-way relay fading channels," in *Proc. IEEE Int. Conf. Comm. (ICC)*, May 2010.
- [19] E. Biglieri, J. Proakis, and S. Shamai, "Fading channels: information-theoretic and communications aspects," *IEEE Trans. Inform. Theory*, vol. 44, no. 6, pp. 2619–2692, October 1998.
- [20] G. Ungerboeck, "Channel coding with multilevel/phase signals," *IEEE Trans. Inform. Theory*, vol. IT-28, no. 1, pp. 55–67, January 1982.
- [21] D. J. C. Mackay, "Encyclopedia of sparse graph codes," Sep. 2009. [Online]. Available: <http://www.inference.phy.cam.ac.uk/mackay/codes>